Intrinsic Structure−Reactivity Relationships in Gas-Phase Transacylation Reactions: Identity Exchange of Substituted Benzoyl Chlorides with Chloride Ion

Meili Zhong and John I. Brauman*

Contribution from the Department of Chemistry, Stanford University, Stanford, California 94305-5080

Received September 8, 1997

Abstract: The identity transacylation reactions of chloride with several substituted benzoyl chlorides, $Cl^- + XC_6H_4COCl$, have been investigated. For X = p-CH_3, m-CH_3, H, m-OCH_3, m-F, and m-CF_3, the complexation energies of the ion−molecule intermediates and the rate constants of the reactions have been measured. The energy difference between the reactants and the transition state, ΔE_{diff}, has been obtained through RRKM modeling of the experimental rate constants. Quantum calculations on the structures and energetics of the complex intermediates and transition states have been conducted, and the calculated energetics of the surface are reasonably consistent with the experimental results. We find that the substituent on the neutral electrophile affects both the complexation energy and ΔE_{diff}, but in a different manner; the energy difference between the complex and the transition state does not remain constant for the entire system. This is different from the substituted benzyl chloride S_N2 system, in which the intrinsic activation energy remains constant for the entire series, but can be explained in terms of the structures of the complex and transition state for these reactions.

Introduction

Nucleophilic displacement reactions at carbonyl centers are among the most studied reactions because of the importance of the carbonyl functional group in both chemistry and biochemistry. In solution, the mechanistic details of acyl transfer reactions have been extensively investigated.[1−3] Many experiments support the proposition that carbonyl addition−elimination reactions proceed through a covalently bound, tetrahedral intermediate.[1,2,4−8] These studies, however, reflect effects of the solvents and counterions in solution. Subsequently, both experimental work in the gas phase and theoretical work have been performed to explore the intrinsic properties of transacylation reactions. Of particular interest are the parameters that determine whether the tetrahedral structure is an intermediate or a transition state on the potential energy surface. We have proposed that the electron affinity of the ionic reactant plays a very important role in determining the relative stability of the tetrahedral structure,[9−11] and that the transition state has a tetrahedral structure in many transacylation reactions. The effect of neutral substrate structure on the reactivity in gas-phase transacylations, however, has been less studied. Complications associated with multiple reaction channels in previously studied

reactions, difficulties in the equilibrium measurements, and a shortage of theoretical resources have hindered the full characterization of the effect of substrate structure on the potential energy surface.

In an attempt to understand more detail about the mechanistic chemistry and the intrinsic effect of the substrate structure on the potential energy surface of the gas-phase carbonyl transacylation reaction, we have studied experimentally and theoretically the transacylation reactions of a series of substituted benzoyl chlorides (eq 1).
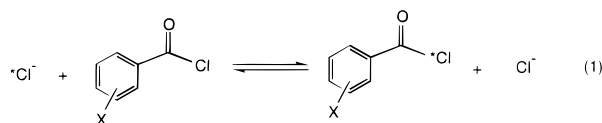
The identity chloride transacylation reactions have been chosen because (1) the substituent in the benzene ring can be a probe to study the electronic effect on the reaction center, (2) these reactions are thermoneutral and complications associated with the thermodynamic driving force effect are eliminated, (3) the steric effect is constant, (4) there are no other reaction channels available, and (5) the reaction rates and the stabilities of the intermediate complexes are within the measurement capabilities of our instrument.[12]

We have measured the rates of a series of chloride carbonyl transacylation reactions (eq 1) using Fourier transform mass spectroscopy. The substituents are X = p-CH_3, m-CH_3, H, m-OCH_3, m-F, and m-CF_3. Using these experimental data, we employed microcanonical variational transition-state (μVTS) RRKM theory to estimate ΔE_{diff}, the energy difference between the reactants and the transition state. The chloride binding energies of the complexes have also been determined by measuring the equilibrium constants between these complexes

(1) Bender, M. L. *Chem. Rev.* **1960**, *60*, 53.

(2) Jencks, W. P. *Catalysis in Chemistry and Enzymology*; Dover: Mineola, 1987.

(3) March, J. *Advanced Organic Chemistry,* 3rd ed.; John Wiley and Sons: New York, 1985.

(4) Bender, M. L. *J. Am. Chem. Soc.* **1951**, *73*, 1626.

(5) Fedor, L. R.; Bruice, T. C. *J. Am. Chem. Soc.* **1965**, *87*, 4138.

(6) Johnson, S. L. *J. Am. Chem. Soc.* **1964**, *86*, 3819.

(7) Fraenkel, G.; Watson, D. *J. Am. Chem. Soc.* **1975**, *97*, 231.

(8) Hand, E. S.; Jencks, W. P. *J. Am. Chem. Soc.* **1962**, *84*, 3505.

(9) Baer, S.; Brinkman, E. A.; Brauman, J. I. *J. Am. Chem. Soc.* **1991**, *113*, 805.

(10) Wilbur, J. L.; Brauman, J. I. *J. Am. Chem. Soc.* **1994**, *116*, 5839−5846.

(11) Wilbur, J. L.; Brauman, J. I. *J. Am. Chem. Soc.* **1994**, *116*, 9216−9221.

(12) Dodd, J. Ph.D. Dissertation, Stanford University, 1985.

Transacylation Reactions of Cl$^-$ and XC$_6$H$_4$COCl

J. Am. Chem. Soc., Vol. 121, No. 11, 1999 2509

and some chloride complexes of known stability. In addition, we carried out AM1 and ab initio quantum calculations to study the reactant, complex, and transition-state structures.

We report in this paper the effect of substrate structure on ΔE_{diff} and the binding energy of the intermediate complex for the reaction in eq 1. We find that the complexation energy and ΔE_{diff} both change with substitution on the benzene ring. These results are consistent with our previous suggestions that the transition state has a tetrahedral structure. In conjunction with quantum calculations, they also suggest that the structure of the complex is rather different from a simple attachment of the chloride to the backside of the carbonyl group.

Experimental Section

Materials. All chemicals used in this study were purchased from Aldrich. They were purified by distillation prior to use. The samples were subjected to multiple freeze−pump−thaw cycles before introduction into the ion cyclotron resonance cell.

Instrumentation. All the experiments were performed in a Fourier transform IonSpec OMEGA ion cyclotron resonance (FT-ICR) spectrometer equipped with impulse excitation. Details of the experimental apparatus can be found elsewhere.[13,14] Briefly, the ICR consists of a 2 × 2 × 2 in. cubic cell, constructed from six stainless steel plates mounted on Vespel rods. All ions were trapped with magnetic fields at about 0.6 T. Neutral samples were admitted to the high-vacuum can by means of Varian leak valves.

During the experiments, pressures of neutral species within the ICR cell were monitored with an ion gauge (Varian 844) which was calibrated against a capacitance manometer (MKS 170 Baratron with a 315 BH-1 head). Typical operating pressures were between 10^{-7} and 10^{-6} Torr. Primary ions were generated by electron impact on neutral precursors. The kinetic energy of the incident electrons was controlled by varying the potential applied to the filament and the bias on the trapping plates. Typical operating current and voltage for the filament were 2−3 A and 1−3 V, respectively. Standard notched ejection techniques were used to remove unwanted ions from the ICR cell and thereby isolate the ions of interest. All experiments were carried out at a temperature estimated to be 350 K.[15]

Data Collection. Kinetics. The reaction in eq 1 was studied by direct observation of isotope exchange. Cl$^-$ was generated directly from reactive substrates by dissociative electron attachment (eq 2). The proper
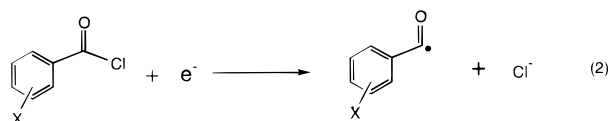
isotope ratio (^{35}Cl/^{37}Cl ≈ 3) was observed over a large time interval before each kinetic run. One of the isotopes of Cl$^-$ was ejected, leaving only the other isotope. The ion signals of both isotopes of Cl$^-$ were measured using signal averaging (50−100 times) until the equilibrium chloride isotope ratio was reached, or for as long as possible (ca. 1000−3000 ms depending on the pressure of the neutral in the cell). The ion signals were monitored at 10 different increments of time. Kinetic runs for each reaction system were carried out at a variety of different pressures, and data were collected on different days. Rate constants were reproducible to ±10%; the major source of error in the kinetic measurements is the pressure measurements, which are accurate to within 20−30%.

Equilibrium Measurements. Typical operating pressures were between 10^{-6} and 10^{-7} Torr. At these pressures, bimolecular collisions occur once every 1−10 ms. In this pressure range there is no simple mechanism for removal of excess energy of a bimolecular collision complex, since the lifetime of a bimolecular collision complex is usually less than microseconds. Thus, intermediate complexes cannot generally be observed. The method used here for generation of the chloride ion/

(13) Wilbur, J. L. Ph.D. Dissertation, Stanford University, 1993.
(14) Zhong, M.; Brauman, J. I. *J. Am. Chem. Soc.* **1996**, *118*, 636.
(15) Han, C. C.; Brauman, J. I. *J. Am. Chem. Soc.* **1989**, *111*, 6491.

Table 1. Kinetic Data for the Reactions *Cl$^-$ + XC$_6$H$_4$COCl → Cl$^-$ + XC$_6$H$_4$CO*Cl

| substituent	$k_{obs} \times 10^{-10}$ (cm^3 s^{-1})	k_{cap}(SC) $\times 10^{-9}$ (cm^3 s^{-1})[a]	Φ (%)	ΔE_{diff} (kcal/mol)	σ^b
p-CH$_3$	0.86	3.89	2.2	−4.0	−0.14
m-CH$_3$	2.69	3.62	7.4	−5.8	−0.06
H	3.4	3.50	9.7	−5.9	0.00
m-OCH$_3$	5.46	3.01	18.1	−8.3	0.10
m-F	7.9	2.83	27.9	−8.8	0.34
m-CF$_3$	11.2	2.92	38.3	−11.0	0.46

[a] In the capture rate calculation, dipole moments and moments of inertia were obtained from AM1 calculations (discussed later) and molecular polarizabilities were calculated using an empirical relation (Miller, K. J.; Savchik, J. A. *J. Am. Chem. Soc.* **1979**, *101*, 7206). [b] Hammett σ constants taken from ref 3.

Scheme 1
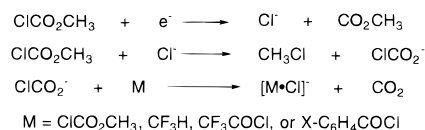
neutral complex is shown in Scheme 1. Chloride-substituted benzoyl chloride complexes were formed and stabilized by loss of CO$_2$. Equilibrium measurements, eq 3, were carried out with standard
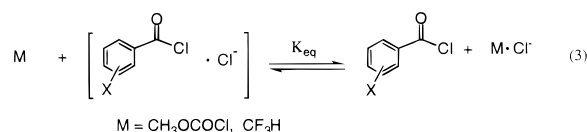
compounds whose chloride affinities are close to those of our substituted complexes. Thus, ClCO$_2$CH$_3$·Cl$^-$ was used for low chloride affinity complexes, and CF$_3$H·Cl$^-$ and CF$_3$COCl·Cl$^-$ were used for high chloride affinity complexes.[16] Ion signals were measured and averaged (50−100 times) at each time increment until equilibrium was reached between the complexes in the cell. The equilibrium constants for reactions between the standards and the benzoyl chloride complexes were determined from the ratio of the complex ions and the pressures of the neutral compounds. The equilibria among these chloride and benzoyl chloride complexes were also measured for comparison. These equilibrium constant measurements were performed at a variety of pressures and on different days.

Results

Kinetics. The rates of these chloride identical exchange reactions have been determined using eq 4,[17,18] where R_t is the

$$\ln\left[\frac{R_t - R_\infty}{R_t + 1}\right] = -k_{obs}Pt \qquad (4)$$

ratio of ion intensities ([^{35}Cl/^{37}Cl] at time t, R_∞ is the natural isotope ratio of ^{35}Cl/^{37}Cl, k_{obs} is the observed rate constant, and P is the pressure of the reactant. Since the reactant and product ions have similar masses, problems resulting from ion loss should be eliminated. Rate constants were reproducible to ±10%. The observed rate constants are listed in Table 1. The capture rate constants, k_{cap}, calculated with the Su−Chesnavich method,[19] and the reaction efficiencies, ($\Phi = k_{obs}/k_{cap}$), are also listed in Table 1.

Thermodynamics. The complexation energies, $\Delta H_{complex}$, for formation of [X−C$_6$H$_5$COCl·Cl$^-$], eq 5, have been determined

(16) Larson, J. W.; McMahon, T. B. *Can. J. Chem.* **1984**, *62*, 675.
(17) Eyler, J. R.; Richardson, D. E. *J. Am. Chem. Soc.* **1985**, *107*, 6130.
(18) Wladkowski, B. D.; Wilbur, J. L.; Brauman, J. I. *J. Am. Chem. Soc.* **1994**, *116*, 2471.
(19) Su, T.; Chesnavich, W. J. *J. Chem. Phys.* **1982**, *76*, 5183.

Table 2. Equilibrium Data for X·Cl⁻ + CH₃OCOCl → CH₃OCOCl·Cl⁻ + X and Complexation Energies of the Chloride Neutral Complexes

X	$\Delta G°_{rel}$ (kcal mol⁻¹)	$\Delta S°_{rel}$ (cal mol⁻¹K⁻¹)[a]	$\Delta H°_{rel}$ (kcal mol⁻¹)	$\Delta H_{complex}$ (kcal mol⁻¹)
p-CH₃C₆H₄COCl	1.03 ± 0.01	0.9	1.4	−15.5
m-CH₃C₆H₄COCl	2.17 ± 0.06	1.0	2.5	−16.6
C₆H₅COCl	1.66 ± 0.10	2.6	2.6	−16.7
m-OCH₃C₆H₄COCl	5.36 ± 0.05	1.8	6.0	−20.1
m-FC₆H₄COCl	4.18 ± 0.06	−0.2	4.1	−18.2
m-CF₃C₆H₄COCl	5.47 ± 0.04	0.6	5.7	−19.8
CF₃H[b]	2.0	0.9	2.3	−16.4
ClCO₂CH₃[b]	0	0	0	−14.1

[a] Entropy calculated from statistical thermodynamic relationships using geometries and frequencies obtained from semiempirical AM1 calculations.
[b] Reference 16.

$$(5)$$
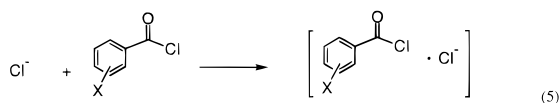
from equilibrium measurements relative to standard chloride complexes, eq 3. The standards used here are CH₃OCOCl·Cl⁻ and CF₃H·Cl⁻ whose complexation energies have been determined by Larson and McMahon.[16]

The free energy changes for the equilibria in eq 3, $\Delta G°_{rel}$, have been obtained by measuring the equilibrium constant K_{eq} between the complex of chloride with the substituted benzoyl chlorides and the standard complexes from $\Delta G°_{rel} = -RT \ln K_{eq}$. The subscript "rel" is used here because the measured free energy changes of eq 3 are actually complexation free energies of [X−C₆H₅COCl·Cl⁻] relative to the standards. We have also measured equilibria of these chloride and substituted benzoyl chloride complexes relative to each other, and the obtained relative free energies agree with the ones from the measurement with the standard CH₃OCOCl·Cl⁻ and CF₃H·Cl⁻ complexes to within 5%.

Since we are interested in the enthalpy changes in eq 3, $\Delta H°_{rel}$, the entropy changes $\Delta S°_{rel}$ are needed. Larson and McMahon used a statistical thermodynamic approximation in which the geometry was roughly estimated and the vibrational entropy change was neglected. Wladkowski et al.[18] used the results of quantum calculations to obtain the geometry and vibrational frequencies and calculate the entropy changes in the S_N2 reaction system. In our work here, we have also obtained geometries for the reactants and complexes and the vibrational frequencies from quantum calculations (discussed later). There is only a very small difference between McMahon's entropies and those obtained with our method.

From the free energy change and entropy change data, the enthalpy changes in eq 3, $\Delta H°_{rel}$, were derived from $\Delta H°_{rel} = \Delta G°_{rel} + T\Delta S°_{rel}$. Since $\Delta H°_{rel}$ is the complexation energy of the complexes [X−C₆H₅COCl·Cl⁻] relative to the standards, the absolute complexation energies of our complexes, $\Delta H_{complex}$, eq 5, were obtained by subtracting $\Delta H°_{rel}$ from the complexation energies of the standard complexes which were taken from Larson and McMahon. The values of free energy change, entropy change, and enthalpy change in eq 3 and the complexation energies of the chloride/neutral complexes are listed in Table 2.

Equilibrium constants were reproducible to within 10%. Errors in $\Delta H_{complex}$ have three primary sources. First, there is a small error in the relative free energy $\Delta G°_{rel}$ measurements due to uncertainty in the relative pressure measurement. The errors in absolute pressure should cancel. Second, the reference complexation energies for CH₃OCOCl·Cl⁻ and CF₃H·Cl⁻ contain some error. Relative values, however, are likely to be accurate. Third, a small error is introduced in the calculation of

Scheme 2
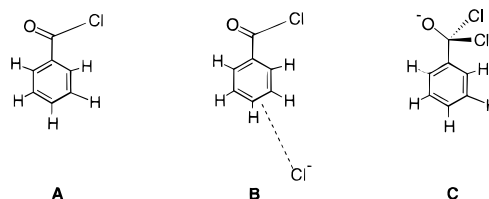
Scheme 3
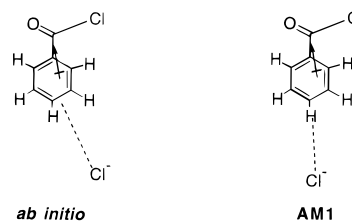
the entropy change. In Table 2, the standard deviation from the mean of all measurements taken is listed.

Quantum Calculations. The primary purpose of the quantum calculations is to determine reasonably accurate structural, energetic, and spectroscopic estimates of the reaction systems. These data are used in the RRKM analysis to obtain ΔE_{diff} from the experimental data. The structures and geometries of the reactants, ion−molecule complex, and transition state for the unsubstituted benzoyl chloride system have been investigated using ab initio molecular orbital calculations at the 6-31+G* level.[20] The vibrational frequencies and rotational constants are listed in Table 3. The structures (**A**, reactant; **B**, complex; and **C**, transition state) are shown in Scheme 2. The energies for the reactants, the complex, and the transition state were also obtained from an ab initio calculation at the MP2/6-31+G*// 6-31+G* level. The calculated surface energetics (including zero-point energy) for the benzoyl chloride reaction system give −6.6 kcal/mol for ΔE_{diff} and −15.4 kcal/mol for ΔE_{well} in good agreement with the experimental values.

For the ion−dipole complex of chloride with benzoyl chloride, the local minimum found in the 6-31+G* calculation is one in which chloride ion binds to the benzene ring close to the dipole axis, rather than one in which chloride ion binds to the carbonyl group, the reaction center (Scheme 3). AM1 MOPAC[21] was also used to calculate the properties of the complex. As shown in Scheme 3, the structure of the complex calculated by AM1 is similar to that from the ab initio calculation; both give structures in which the chloride binds close to the dipole axis. The structural information for the substituted complexes was obtained only from AM1 MOPAC

(20) Frisch, M. J.; et al. *Gaussian 94, Revision C.3*; Gaussian, Inc: Pittsburgh, PA, 1995.
(21) Stewart, J. J. P. *MOPAC 6.00,* No. 455, 1990.

Table 3. Parameters Used in the RRKM Analysis of the Reaction of Cl⁻ + C₆H₅COCl, as a Representative Example

dissociation transition state Cl⁻···C₆H₅COCl	complex [Cl⁻·C₆H₅COCl]	transition state [Cl·C₆H₅COCl]⁻ †	dissociation transition state Cl⁻···C₆H₅COCl	complex [Cl⁻·C₆H₅COCl]	transition state [Cl·C₆H₅COCl]⁻ †
$v_i{}^a$	22	314i	$v_i{}^a$		
38ᵇ	34ᵇ	43ᵇ	1028 [1028] (1175)	1010	999
151 [163] (144)	45	102	1070 [1078] (1193)	1014	1006
186 [194] (188)	80	118	1109 [1162] (1200)	1064	1011
311 [318] (342)	155	175	1169 [1175] (1234)	1071	1061
406 [418] (367)	187	199	1184 [1206] (1316)	1118	1100
422 [418] (416)	309	241	1216 [1315] (1381)	1159	1147
424 [500] (461)	403	313	1325 [1321] (1415)	1181	1165
499 [509] (554)	416	407	1446 [1455] (1569)	1222	1206
606 [615] (599)	419	421	1493 [1483] (1612)	1322	1317
650 [650] (657)	492	462	1596 [1582] (1760)	1442	1442
664 [673] (709)	605	546	1613 [1599] (1775)	1486	1491
683 [692] (754)	645	597	1811 [1776] (2037)	1587	1596
784 [777] (822)	652	612	3029 [3010] (3165)	1597	1615
863 [848] (891)	682	686	3042 [3030] (3172)	1790	1764
873 [875] (969)	793	762	3051 [3078] (3180)	3027	3002
971 [890] (970)	858	785	3071 [3078] (3188)	3054	3017
980 [976] (994)	866	853	3081 [3078] (3196)	3060	3030
1012 [989] (1014)	977	947		3062	3063
1013 [1003] (1110)	980	978		3076	3087
B_{int}(tors), $\sigma_i{}^c$ 1.055, 1 (1)	1.055, 1 (1)	0.937, 1 (1)	B_{ext}(act), $\sigma_i{}^c$ 0.1070, 1 (1)	0.0742, 1 (1)	0.0497, 1 (1)
B_{int}(hind), $\sigma_i{}^c$ 0.0293, 1 (2)			B_{ext}(inact), $\sigma_i{}^c$ d	0.0100, 1 (2)	0.0213, 1 (2)

ᵃ Values in brackets are the experimental frequencies (Condit, D. A.; Craven, S. M.; Katon, J. E. *Appl. Spectrosc.* **1974**, *28*, 420), and values in parentheses are the frequencies from AM1 calculations. ᵇ Treated as torsional rotations. ᶜ Rotational constants (cm⁻¹) obtained from ab initio calculations; dimensionality is given in parentheses. ᵈ The value of the moment of inertia and rotational constant of the 2-dimensional external inactive rotor for the loose transition state is a function of the separation of the centers of mass of the two species: (r(C−Cl) in anstroms, $2D − B_{ext}$(inact) in inverse centimeters) 6.5, 0.009 83; 7.4, 0.007 90; 8.4, 0.006 46; 10.3, 0.004 52; 12.3, 0.003 32; 14.0, 0.002 53; 20.2, 0.001 32; 25.1, 0.000 868; 35.1, 0.000 468; 45, 0.000 288.

Table 4. Thermodynamic Data from AM1 Calculations for the Complexation Reaction Cl⁻ + XC₆H₄COCl → [Cl⁻·XC₆H₄COCl]

substituent	$\Delta H°$ (kcal mol⁻¹) (AM1)	substituent	$\Delta H°$ (kcal mol⁻¹) (AM1)
p-CH₃	−17.5	*m*-OCH₃	−22.0
m-CH₃	−16.7	*m*-F	−20.0
H	−18.3	*m*-CF₃	−23.0

calculations. Table 4 lists heats of complexation obtained from the AM1 calculations.

The transition state of the chloride benzoyl chloride reaction system is found to be the tetrahedral structure at the 6-31+G* level (Scheme 2, **C**). The oxygen lies in the same plane as the benzene ring, and the C−Cl bond length is 2.13 Å. The AM1 calculation, however, failed to reproduce this result; the tetrahedral structure is not a transition state at the AM1 level.[22]

Data Analysis: RRKM Modeling. RRKM analysis has been used to estimate the effective activation barriers for the transacylation reactions from the kinetic experimental results listed in Table 1. We used the RRKM program HYDRA[23] which has been applied for modeling the kinetics of some S_N2 and addition−elimination systems.[18,23−27] Details of the modeling

(22) AM1 calculations found no negative vibrational frequency for the tetrahedral structure. Instead, the energy of the tetrahedral structure is even lower than that of the ion−dipole complex. In the ion−dipole complex, most of the charge is on the chloride, while in the tetrahedral structure, most of the charge is on the oxygen. This discrepancy is not surprising since AM1 grossly underestimates the stability of chloride anion relative to alkoxide anions. For example, AM1 calculations underestimate the heat of formation of Cl⁻ by as much as 17 kcal/mol but underestimate that of CH₃O⁻ by only 5 kcal/mol.
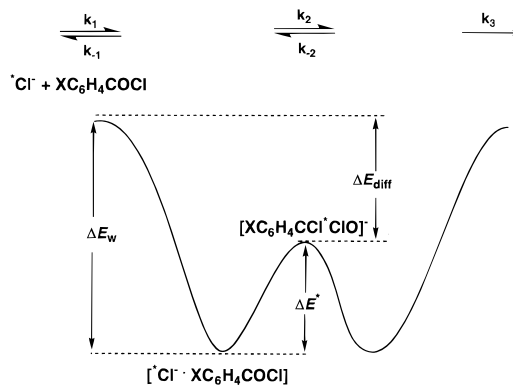
(23) Wladkowski, B. D.; Lim, K. F.; Allen, W. D.; Brauman, J. I. *J. Am. Chem. Soc.* **1992**, *114*, 9136.

(24) Viggiano, A. A.; Morris, R. A.; Su, T.; Wladowski, B. D.; Craig, S. L.; Zhong, M.; Brauman, J. I. *J. Am. Chem. Soc.* **1994**, *116*, 2213.

(25) Craig, S. L.; Brauman, J. I. *Science* **1997**, *276*, 1536−1538.

(26) Craig, S. L.; Zhong, M.; Brauman, J. I. *J. Phys. Chem.* **1996**, *101*, 19.

(27) Craig, S. L.; Zhong, M.; Brauman, J. I. Manuscript in preparation.

Figure 1. Generalized potential energy surface for gas-phase carbonyl addition−elimination reactions.

may be found in the previous work.[23] A brief description is presented here.

A double well potential energy surface is used to model the gas-phase transacylation reaction, Figure 1. As shown in Figure 1, the reactants come together to form a chemically activated complex [XC₆H₄COCl·*Cl⁻]. This complex can either dissociate back to the reactants or pass through the transition state [XC₆H₄COCl*Cl⁻] to give the product complex [XC₆H₄-CO*Cl·Cl⁻] which can then return to the reactant complex or dissociate to products.

The overall reaction rate coefficient for a symmetric thermoneutral reaction ($k_2 = k_{−2}$; $k_3 = k_{−1}$) in the steady-state approximation is

$$k_{obs} = \frac{k_1 k_2}{k_{−1} + 2k_2} \qquad (6)$$

In eq 6, k_1 is the capture rate constant, $k_{−1}$ is the dissociation rate constant of the reactant complex, and k_2 is the reactant

complex reaction rate constant. A more convenient quantity is the macroscopic efficiency Φ:

$$\Phi = \frac{k_{obs}}{k_1} = \frac{k_2}{k_{-1} + 2k_2} \qquad (7)$$

As shown in eq 7, Φ depends only on k_2 and k_{-1}, the unimolecular rate constants for the reactant complex.

The macroscopic efficiency is the sum of its microscopic counterparts, weighted according to the energy and angular momentum distribution of the reactant complex, $F(E,J)$.

$$\Phi = \int\int \Phi(E,J)\, F(E,J)\, dE\, dJ \qquad (8)$$

where $F(E,J)$ represents the distribution of activated complexes initially formed with energy E and total angular momentum J. The detailed discussion of $F(E,J)$ can be found elsewhere.[23] The microscopic efficiency $\Phi(E,J)$ is determined from microscopic rate coefficients, $k_i(E,J)$, eq 9.

$$\Phi(E,J) = \frac{k_2(E,J)}{k_{-1}(E,J) + 2k_2(E,J)} \qquad (9)$$

The rate constants in eq 9 can be calculated using unimolecular reaction rate theory with the microcanonical variational transition-state approximation (μVTST) as given in eq 10.[28−33]

$$k(E,J) = \sigma \frac{\int_0^{\epsilon(J;R^*)} \rho_{\mu VTST}^\dagger(\epsilon')\, d\epsilon' k_1}{h\rho[\epsilon(J;R_e)]} = \sigma \frac{W_{\mu VTST}^\dagger[\epsilon(J;R^*)]}{h\rho[\epsilon(J;R_e)]} \qquad (10)$$

σ is the reaction path degeneracy, R denotes the reaction coordinate, defined as the separation of the center of mass of the two reactants, $\epsilon(J;R) = E - V(R) - E_r(J;R)$, $W_{\mu VTST}^\dagger[E,J]$ is the accessible sum of states at the transition state (located at $R = R^*$) for each (E,J) channel, and $\rho[\epsilon(J;R_e)]$ is the corresponding density of states for the appropriate ion−molecule complex (for which $R = R_e$). The functions $V(R)$ and $E_r(J;R)$ represent the potential energy and orbital rotational energy, respectively, along the reaction coordinate. $V(R)$ can be modeled using a simple electrostatic model incorporating experimental molecular parameters for each neutral (i.e., polarizability and dipole moment).[23] $E_r(J;R)$ is determined using a diatomic approximation. In the evaluation of k_{-1}, the location of the "loose" transition state in eq 10 is chosen so that $W^\dagger$ is minimized:[34]

$$W_{\mu VTST}^\dagger(E,J) = \min_R\{W^+[\epsilon(J;R)]\} \qquad (11)$$

where the minimization is performed over all possible values of R in the entrance channel for each E and J.

For the determination of k_2, R^* in eq 10 is selected to coincide with the "tight" transition state. The "tight" transition state is treated as a tetrahedral structure. Although experimental evi-

dence for the transition-state structure on a double well potential energy surface is not available for the specific reaction in eq 1, considerable indirect evidence suggests that the transition state has a tetrahedral structure (see the Discussion).

In the μVTST-RRKM modeling, data for the unsubstituted benzoyl chloride system were obtained from quantum ab initio calculations and are given in Table 3 as a representative example. The scaled vibrational frequencies and rotational constants for the reactants, reaction complex, and transition state are listed. Also listed in Table 3 are the scaled vibrational frequencies of benzoyl chloride from semiempirical AM1 calculations and experiments. Reasonably good agreement is found among the experimental, ab initio, and AM1 frequencies for the benzoyl chloride system. Data for other systems were obtained by modifying the frequencies of the unsubstituted benzoyl chloride system according to differences between the unsubstituted and substituted benzoyl chlorides calculated using the AM1 model. Since the substituent groups are far from the reaction center, the additional vibrations in the substituted compounds have been treated as local modes and their frequencies simply added to the frequencies of the complex and the transition state for benzoyl chloride. In effect, this increases both $W^\dagger$ and ρ appropriately to account for the additional oscillators. Other frequencies shift slightly and have been adjusted accordingly. We expect that errors introduced by this procedure will be modest and have only a minimal effect on the calculation of $k(E,J)$.

In the μVTST-RRKM modeling, using the data described above, we can obtain the macroscopic efficiency for a given temperature after averaging over the appropriate chemically activated energy and angular momentum distribution. Then, we determine the value of ΔE_{diff} for which the calculated reaction efficiency matches the experimental reaction efficiency at 350 K, the temperature at which our experiments were performed. The experimental reaction efficiency, $\Phi = k_{obs}/k_1$ as shown in eq 8, can be obtained after the capture rate k_1 is determined. In this study, we calculated the capture rate k_1 using the model of Su and Chesnavich which has been shown to give accurate results.[19]

Discussion

Transacylation reactions involving ketones, aldehydes, and carboxylic acid derivatives have been extensively studied in solution. These reactions are thought to proceed through an addition−elimination mechanism in which the tetrahedral structure is an intermediate as shown in eq 12.[4−6,8,35−39] Whereas
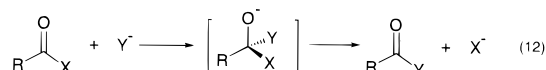
the tetrahedral structure is an intermediate in the condensed phase, whether it is a minimum or a transition state in the gas phase depends on the properties of the reactants. Asubiojo and Brauman observed that the rates of many carbonyl addition−elimination reactions in the gas phase were much slower than collision rates.[40] This led them to propose a double well surface model in which the minima of the surface are unsymmetrical ion−dipole complexes while the tetrahedral structure is the

(28) Smith, S. C. *J. Chem. Phys.* **1992**, *97*, 2406.

(29) Robinson, P. J.; Holbrook, K. A. *Unimolecular Reactions*; Interscience: London, 1972.

(30) Forst, W. *Theory of Unimolecular Reactions*; Academic Press: New York, 1973.

(31) Gilbert, R. G.; Smith, S. C. *Theory of Unimolecular and Recombination Reactions*; Blackwells Scientific: Oxford, 1990.

(32) Trular, D. G.; Hase, W. L.; Hynes, J. T. *J. Phys. Chem.* **1983**, *87*, 2664.

(33) Steinfeld, J. I.; Francisco, J. S.; Hase, W. L. *Chemical Kinetics and Dynamics*; Prentice Hall: Englewood Cliffs, NJ, 1989.

(34) Garrett, B. C.; Truhlar, D. G. *J. Chem. Phys.* **1979**, *70*, 1593.

(35) Zerner, B.; Bender, M. L. *J. Am. Chem. Soc.* **1961**, *83*, 2267.

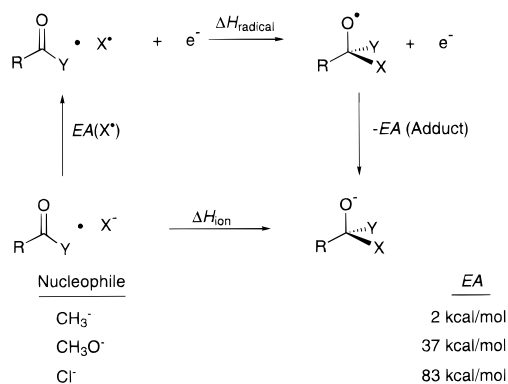(36) Mader, P. M. *J. Am. Chem. Soc.* **1965**, *73*, 3191.

(37) Schowen, R. L.; Jayaraman, H.; Kershner, L. *J. Am. Chem. Soc.* **1966**, *88*, 3373.

(38) Eriksson, S. O.; Holst, C. *Acta Chem. Scand.* **1966**, *20*, 1892.

(39) Bender, M. L. *J. Am. Chem. Soc.* **1953**, *75*, 5986.

(40) Asubiojo, O. I.; Brauman, J. I. *J. Am. Chem. Soc.* **1979**, *101*, 3175.

Scheme 4

Nucleophile	*EA*
CH_3^-	2 kcal/mol
CH_3O^-	37 kcal/mol
Cl^-	83 kcal/mol

transition state. The relative stability of various tetrahedral addition products, however, is quite variable. The enthalpy of addition ΔH_{ion} depends strongly on the relative electron binding energies of the nucleophile and the tetrahedral adduct, Scheme 4.[9] If $\Delta H_{radical}$ is relatively small, which is the case for many nucleophiles, including alkyls, chloride, and alkoxides, the energy of formation of the adduct depends mostly on the difference between the electron binding energy of the nucleophile ($-EA$) and the adduct. In the case of a nucleophile with a very low electron binding energy (e.g., H^-, CH_3^-) the tetrahedral adduct is expected to be stable. In the case of a nucleophile with a very high electron binding energy (e.g., Cl^-, CN^-), the tetrahedral structure is expected to be high in energy. When the electron binding energy of the nucleophile is comparable to that of the tetrahedral adduct (e.g., OH^-, RO^-), however, the energetics for the formation of the tetrahedral adduct become less clear.

Experimentally, Bohme and co-workers observed a tetrahedral adduct (presumably CH_3O^-) from the reaction of H^- with formaldehyde by using a helium buffer gas to collisionally deactivate the adduct product.[41] McDonald and co-workers also observed a stable tetrahedral adduct from the reaction of CF_3^- with $(CF_3)_2CO$.[42] For nucleophiles such as OH^- and RO^-, both tetrahedral adduct and ion−dipole complexes have been observed. Bowie and Williams reported a stable adduct product from reaction of trifluoroacetate anion with perfluoroacetic anhydride on the basis of its decomposition reactions.[43] Brauman and co-workers found the most stable structure for a deprotonated cyclic hemiacetal anion to be tetrahedral.[9] Nibbering and van der Wel, however, reported that ion−dipole complexes coexisted with the tetrahedral adducts for a series of reactions of methoxide with aldehydes and esters.[44] Larson and McMahon have measured the complex binding energies for F^-, Cl^-, and CN^- with a series of neutral molecules including aldehydes, esters, and ketones.[16,45−47] In most cases, the binding affinities suggested an electrostatic complex. Wilbur and Brauman showed that the intermediate in the reaction of Cl^- with CH_3-$OCOCl$ is an unsymmetrical ion−molecule complex.[10] They also observed that intermediates in the reaction of CN^- with 3,5-difluorobenzoyl chloride were unsymmetrical ion−molecule

complexes and found no evidence for a stable, covalent, tetrahedral adduct.[11] In a theoretical study, Yamabe and Minato predicted an ion−dipole structure for the complex in the reaction of Cl^- and CH_3COCl.[48] Blake and Jorgensen predicted an ion−dipole complex for the reaction of Cl^- with $HCOCl$ and CH_3-$COCl$, and found a double minimum surface for both bimolecular reactions.[49]

There are numerous studies of the structure−reactivity relationships in transacylation reactions in solution, including the influence of nucleophile, leaving group, and substrate structure on reactivity.[3] Electron-withdrawing groups have been shown to increase the rates while electron-donating groups decrease them. A great deal of effort has focused on quantifying electronic effects of substituents through the use of linear free energy (Hammett) relationships.[50−52]

Gas-phase studies that address substituent effects in transacylation reaction systems are much more limited. Asubiojo and Brauman studied a series of transacylation reactions of Cl^- + $RCOCl$.[40] For exothermic transacylation reactions, however, competitive reactions such as proton transfer and elimination reactions can complicate the quantitative study of structure−reactivity relationships. Riveros, Ingemann, and Nibbering[53] studied reactions of F^- with substituted phenyl acetate, and DePuy et al. studied reactions of methoxide with a series of carbonyl neutrals.[54] Since other reaction channels besides the transacylation reaction are available in these systems, the focus was on substituent effects on the product distribution rather than on the transacylation reaction.

We chose this series of chloride exchange reactions because Cl^- has a high electron affinity, and we expect that the tetrahedral structure is the transition state, on the basis of experimental and theoretical results of similar reaction systems. Ab initio calculations of the vibrational frequencies for the parent benzoyl chloride system at different levels including 3-21+G and 6-31+G* show one imaginary vibrational frequency for the tetrahedral structure, indicating that it is indeed a transition state. The geometry changes slightly from 3-21+G to 6-31+G*. As shown in Scheme 2, in the lowest energy conformation of the tetrahedral structure calculated at the 6-31+G* level, the two chlorides are 2.13 Å away from the carbonyl carbon, and the oxygen is in the same plane as the benzene ring. The energy of the tetrahedral structure is calculated to be 6.6 kcal/mol below those of the reactants at the MP2/6-31+G*//6-31+G* level and 8.8 kcal/mol higher than that of the ion−dipole complex.[22]

The energy differences between the reactants and the transition state (tetrahedral structure) for this series of reactions have been obtained through RRKM modeling of experimental kinetic results, Table 1. This energy difference, ΔE_{diff}, is the quantity that directly influences the observed kinetics. The more negative the value of ΔE_{diff}, the lower the barrier, and the higher the reaction efficiency, Table 1. The reaction efficiencies range from 2% (X = *p*-CH₃) to 38% (X = *m*-CF₃), and the values of ΔE_{diff} for this series of reactions range from −4 kcal/mol (X = *p*-CH₃) to −11 kcal/mol (X = *m*-CF₃).

(41) Bohme, D. K.; Mackay, G. I.; Tanner, S. D. *J. Am. Chem. Soc.* **1980**, *102*, 407.

(42) McDonald, R. N.; Chowdhury, A. K. *J. Am. Chem. Soc.* **1983**, *105*, 7267.

(43) Bowie, J. H.; Williams, B. D. *J. Am. Chem. Soc.* **1974**, *27*, 1923.

(44) Nibbering, N. M. M.; van der wel, H. *Recl. Trav. Chim. Pays-Bas.* **1988**, *107*, 479.

(45) Larson, J. W.; McMahon, T. B. *J. Am. Chem. Soc.* **1983**, *105*, 2944.

(46) Larson, J. W.; McMahon, T. B. *J. Am. Chem. Soc.* **1985**, *107*, 766−773.

(47) Larson, J. W.; McMahon, T. B. *J. Am. Chem. Soc.* **1987**, *109*, 6230.

(48) Yamabe, S.; Minato, T. *J. Org. Chem.* **1983**, *48*, 2972.

(49) Blake, J. F.; Jorgensen, W. L. *J. Am. Chem. Soc.* **1987**, *109*, 3856.

(50) Hammett, L. P. *J. Chem. Educ.* **1966**, *43*, 464.

(51) Hammett, L. P. *Physical Organic Chemistry,* 2nd ed.; McGraw-Hill: New York, 1970.

(52) Jaffé, H. H. *Chem. Rev.* **1953**, *53*, 191.

(53) Riveros, J. M.; Ingemann, S.; Nibbering, N. M. M. *J. Chem. Soc., Perkin Trans. 2* **1991**, 1985.

(54) DePuy, C. H.; Grabowski, J. J.; Bierbaum, V. M.; Ingemann, S.; Nibbering, N. M. M. *J. Am. Chem. Soc.* **1985**, *107*, 1093.
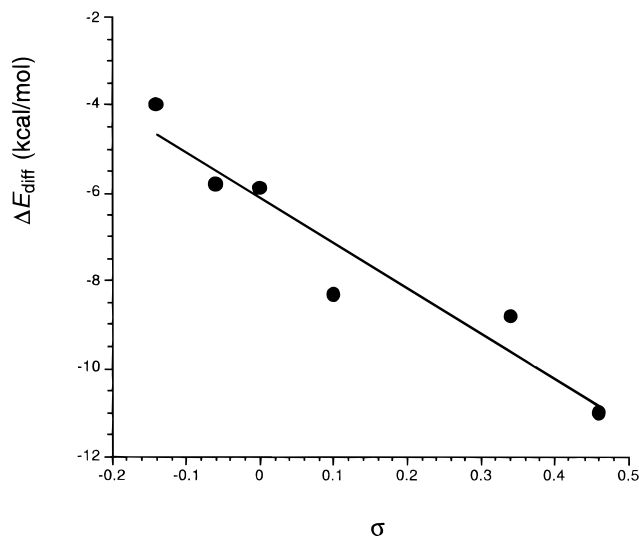
Figure 2. Activation energies relative to separated reactants, ΔE_{diff}, vs Hammett σ constants. The least-squares line is based on all the data.

Figure 3. Complexation energies, ΔE_{w}, vs Hammett σ constants. The least-squares line does not include X = *m*-OCH$_3$.

It is clear that the substituents in the benzene ring of benzoyl chlorides affect ΔE_{diff}, and therefore the rate efficiency. Since there are no other side reactions and the steric effect is constant throughout this series, the electronic effect must be critical in determining ΔE_{diff}. Hammett σ constants, which characterize the substituent electronic effect for the ionization of benzoic acids in water, are listed along with the kinetic data in Table 1. The experimental ΔE_{diff} is plotted versus σ in Figure 2. ΔE_{diff} becomes more negative as the electron-withdrawing character of the substituents increases: the slope of the plot is -10.

As shown in Scheme 3, the local minimum for the ion–molecule complex from the ab initio calculation is one in which Cl$^-$ binds to the benzene ring close to the dipole axis, rather than the carbonyl group. This can be compared with the results of ab initio calculations by Jorgensen et al. on the complex of chloride and CH$_3$COCl. They found the minimum for that complex is one in which chloride sits about 3.29 Å from the backside of the methyl carbon along the dipole axis.[49]

We also used AM1 calculations to obtain the structure of the complex. As shown in Scheme 3, the structure obtained from the AM1 calculations is similar to the one from the ab initio calculation, in which chloride binds to the benzene ring, away from the carbonyl group. Because AM1 and ab initio calculations give comparable results for the complex, we have used AM1 to calculate the structures of the complexes for other substituted benzoyl chloride systems. All of the local minima show a structure similar to that of the Cl$^-$·C$_6$H$_5$COCl complex: chloride binds along the dipole axis near a hydrogen on the benzene ring.

The experimental chloride binding energies for the formation of the intermediate ion–molecule complexes, Cl$^-$ + XC$_6$H$_4$COCl → [Cl$^-$·XC$_6$H$_4$COCl], are listed in Table 2. The complexation energy varies with the substituent of the benzene ring, ranging from -15.5 kcal/mol for X = *p*-CH$_3$ to -20.1 kcal/mol for X = *m*-OCH$_3$. Since all of the experimental equilibrium measurements reflect the stability of the most stable species, the complexation energy should reflect the stability of the most stable ion–dipole complex structure as shown in Scheme 2. The complexation energy of Cl$^-$·C$_6$H$_5$COCl from the ab initio calculation, -15.4 kcal/mol, agrees well with the experimental value, -16.7 kcal/mol.

The complexation energies were also computed directly from the semiempirical AM1 heats of formation data listed in Table
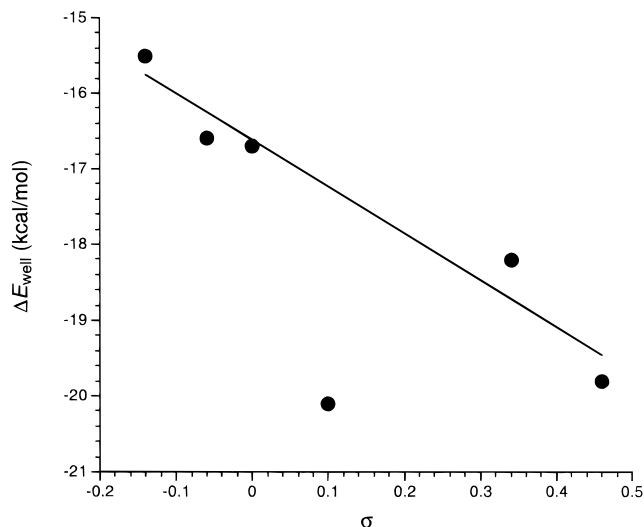
4. The relative results are reasonably consistent with experiment, cf. Table 2, and provide support for the calculated structures of the ion–dipole complexes as a realistic picture of the complexes observed experimentally.

The complexation energy changes with the substituent in this series of reactions. In the quantum calculations, the complex adopts a structure in which the chloride binds along the dipole axis and close to a hydrogen of the benzene ring. Therefore, both the dipole moment of the neutral molecule and the acidity of the hydrogen to which chloride binds closely should play important roles in stabilizing the complex. It has been reported that the electron-withdrawing substituents increase the acidity of the protons in benzene,[55] and Larson and McMahon found a strong correlation between the chloride ion binding energy and the gas-phase acidity of the neutral for Cl$^-$ complexes.[16]

Figure 3 is a plot of the complexation energy vs σ of the substituent. In contrast to the plot for ΔE_{diff}, this plot does not accommodate all the substituents. Electron-withdrawing substituents do stabilize the complex, but for X = *m*-OCH$_3$ the stability is larger than expected on the basis of benzoic acid acidities. Furthermore, the slope is about -6. This shows that the charge stabilization in the complex is not similar to the charge stabilization of ΔE_{diff}, and stabilization by *m*-OCH$_3$ is different from that of the other substituents. This is consistent with the calculations, however, which show that the structure of the complex has the Cl$^-$ interacting with one of the hydrogens of the benzene ring. In contrast to the other substituents, the OCH$_3$ group can adopt additional conformations. For X = *m*-OCH$_3$, the calculated dipole moment for the neutral with the most stable conformation is relatively high (4.6 D),[56] and the complexation energy is also high. We have calculated the complexation energy for X = *m*-OCH$_3$ for different conformations of the OCH$_3$ group and find that the conformation with the smallest dipole moment has a complexation energy about 5 kcal/mol lower than that of the optimal conformation. Figure 4 is a plot of ΔE_{w} vs ΔE_{diff}. The slope is about 6, showing that charge stabilization in the transition state is different from charge stabilization in the complex, and it is clear that the complex of *m*-OCH$_3$ is about 2 kcal/mol more stable than expected on the basis of its kinetic behavior. The structures of the transition states and complexes are very different, and in addition, the

(55) Meot-Ner, M.; Kafafi, S. A. *J. Am. Chem. Soc.* **1988**, *110*, 6297.
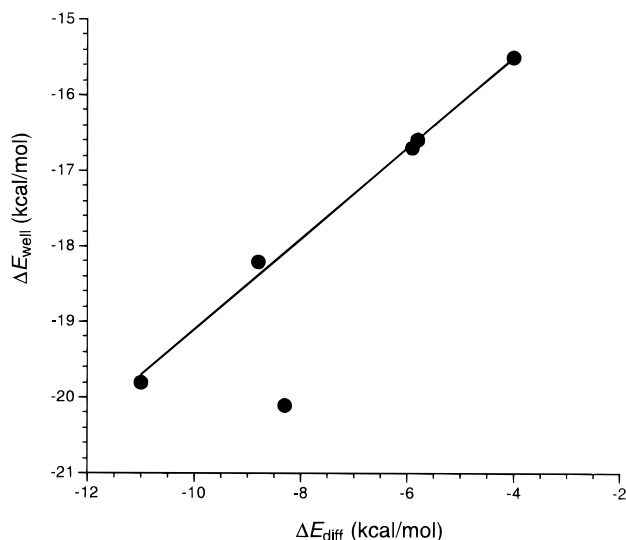(56) This value was obtained from the AM1 MOPAC calculation.

Figure 4. Complexation energies, ΔE_w, vs activation energies relative to separated reactants, ΔE_{diff}. The least-squares line does not include X = m-OCH₃.

Table 5. Intrinsic Activation Energies, ΔE^*, for the Reaction *Cl⁻ + XC₆H₄COCl

substituent	$\Delta E^* = \Delta E_{diff} - \Delta E_w$ (kcal mol⁻¹)	substituent	$\Delta E^* = \Delta E_{diff} - \Delta E_w$ (kcal mol⁻¹)
p-CH₃	12.0	m-OCH₃	12.6
m-CH₃	11.3	m-F	9.9
H	11.0	m-CF₃	9.3

OCH₃ group can adopt a different, more favorable conformation in the complex which provides additional stabilization.

Knowing ΔE_{diff} and the complexation energy ΔE_w, the intrinsic activation energy ΔE^* ($\Delta E^* = \Delta E_{diff} - \Delta E_w$) has effectively been determined. Table 5 shows ΔE^* for all the substituents.

The substituent effects in these reactions provide significant insight about the structures of the complexes and transition states. The plot of ΔE_{diff} vs σ has a slope of about -10. This is comparable to the slope of gas-phase acidities of benzoic acids[57] vs σ and the gas-phase electron affinities of enolate ions[58] vs σ, and it is consistent with the charge being essentially on the oxygen, one atom removed from the benzylic carbon. The plot

(57) McMahon, T. B.; Kebarle, P. *J. Am. Chem. Soc.* **1977**, *99*, 2222−2230.

(58) Jackson, R. L.; Zimmerman, A. H.; Brauman, J. I. *J. Chem. Phys.* **1979**, *71*, 2088−2094.

of ΔE_w vs σ has a slope of about -6. In this case, the stability of the complex is obviously much less sensitive to the substituent. The Cl⁻ is stabilized by the dipole of the carbonyl group and is hydrogen bonded to one of the phenyl protons. The substituent contributes to both of these effects, but to a smaller extent than to the stabilization of the transition state. Because the m-OCH₃ substituent is conformationally mobile, it is able to provide additional stabilization for the complex by adopting a conformation that is different from the optimal transition state conformation. Consequently, m-OCH₃ falls off the plot of ΔE_{diff} vs ΔE_w. Since the slope of the plot of ΔE_{diff} vs ΔE_w is not unity (i.e., the slopes of ΔE_{diff} and ΔE_w vs σ are different), the activation energies, Table 5, are not constant.

The S_N2 reaction provides an interesting contrast.[18] In the S_N2 reaction system, the structure of the transition state and the structure of the complex are very similar. Both ΔE_{diff} and ΔE_w have slopes of about -10 vs σ, consistent with the charge in both the complex and the transition state being roughly one atom removed from the benzylic center. (In neither case is there any significant resonance interaction with the substituent.) The correlation of ΔE_{diff} vs ΔE_w is very good, with a slope of essentially unity. Consequently, the activation energies in the S_N2 reaction system are constant.

Conclusion

The substituent on the neutral electrophile affects both ΔE_{diff} and the complexation energy, ΔE_w, albeit with quantitative differences. ΔE_{diff} becomes more negative as the substituent becomes more electron withdrawing. For the complexation energy, ΔE_w, both the dipole moment of the substituted benzoyl chloride and the acidity of the benzene ring protons play important roles in stabilizing the ion−molecule intermediate complex. Although the transition-state energies and the complexation energies are correlated, the sensitivity of ΔE_{diff} to the substituent is greater than that of ΔE_w, so the difference between ΔE_{diff} and ΔE_w, the intrinsic activation energy, does not remain constant as the substituent is varied. This is different from the substituted benzyl chloride S_N2 system, in which the substituent's ability to stabilize the intermediate complex and the S_N2 transition state is similar.